

4-Carboxyanilinium (2*R*,3*R*)-tartrate and a redetermination of the α -polymorph of 4-aminobenzoic acid

S. Athimoolam* and S. Natarajan

Department of Physics, Madurai Kamaraj University, Madurai 625 021, India
Correspondence e-mail: xrdsofpmku@yahoo.com

Received 2 April 2007

Accepted 7 May 2007

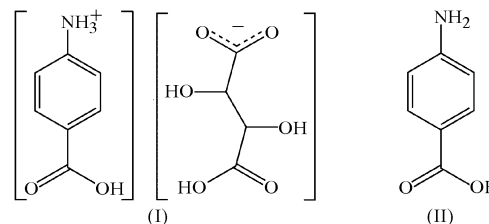
Online 9 August 2007

In the title compounds, 4-carboxyanilinium (2*R*,3*R*)-tartrate, $C_7H_8NO_2^+ \cdot C_4H_5O_6^-$, (I), and 4-aminobenzoic acid, $C_7H_7NO_2$, (II), the carboxyl planes of the 4-carboxyanilinium cations/4-aminobenzoic acid are twisted from the aromatic plane. In (I), the characteristic head-to-tail interactions are observed through the tartrate anions, forming two $C_2^2(7)$ chain motifs propagating parallel to the *a* and *c* axes of the unit cell. Also, the tartrate anions are connected through two primary $C_1^1(6)$ and $C_1^1(7)$ chain motifs, leading to a secondary $R_4^4(22)$ ring motif. In (II), head-to-tail interaction is seen through a discrete $D_1^1(2)$ motif and carboxyl group dimerization is observed through centrosymmetrically related $R_2^2(8)$ motifs around the inversion centres of the unit cell. The crystal structures of both compounds are stabilized by intricate three-dimensional hydrogen-bonding networks. Alternate hydrophobic and hydrophilic layers are observed in (I) as a result of a column-like arrangement of the anions and the aromatic rings of the cations.

Comment

4-Aminobenzoic acid (PABA) is an essential biological molecule, acting as a bacterial cofactor involved in the synthesis of folic acid (Robinson, 1966). PABA is also a starting material in the synthesis of target esters, salts, folic acid, azo dyes and many other organic compounds. It is used in medicine for preparing local anaesthetics and ointments. It helps to protect the skin from sunburn and cancer. Fibrotic skin disorders can also be treated with PABA (Osgood *et al.*, 1982). As PABA can donate and also accept hydrogen, it has proved to be a versatile reagent for structure extension by linear hydrogen-bonding associations, through both the carboxylic acid and amine functional groups. The crystallographic study of PABA compounds was started by Pant (1965), who studied the crystal structure of 4-amino-3,5-dibromobenzoic acid. Later, Lai & Marsh (1967) studied this structure extensively using photographic/visual data. In fact, PABA exists as two different polymorphs, *viz.* the α - and β -forms. The β -form has recently been reinvestigated by Gracin & Fischer (2005). The absence

of diffractometer data for the α -form of this compound, (II), stimulated us to carry out the redetermination of this structure.



PABA complexes such as 4-carboxyphenylammonium nitrate, 4-carboxyphenylammonium perchlorate monohydrate and bis(4-carboxyphenylammonium) sulfate (Athimoolam & Natarajan, 2006), have already been studied in our laboratory to understand their structure–extension properties *via* their linear and cyclic hydrogen-bonding associations. Also, the structures of 4-carboxyanilinium dihydrogenmonoarsenate monohydrate (Tordjman *et al.*, 1988), 2,4,6-trinitrobenzoic acid 4-aminobenzoic acid monohydrate (Lynch *et al.*, 1992), bis(4-aminobenzoic acid)dichlorocadmium(II) (Le Fur & Masse, 1996) and bis(4-aminobenzoic acid)silver(I) nitrate (Wang *et al.*, 2004) have been reported previously. Hu and co-workers have already reported the structure of PABA with tartaric acid in hydrated form (Hu *et al.*, 2002). We present here the crystal structure of an anhydrous form of the PABA–tartaric acid complex, (I).

The asymmetric parts of (I) and (II) consist of two crystallographically independent PABA molecules oriented with angles of 1.7 (3) and 38.4 (1)°, respectively, between them (Figs. 1 and 2). Protonation on the N site of the PABA cation and deprotonation on the –COOH group of the anion in (I) are evident from the C–N and C–O bond distances (Table 1). Twisting out of the carboxyl plane from the aromatic ring plane is a common feature found in PABA complexes [in 27 complexes of PABA adducts in the Cambridge Structural Database (CSD, Version 5.28; Allen, 2002)]. The angles of this

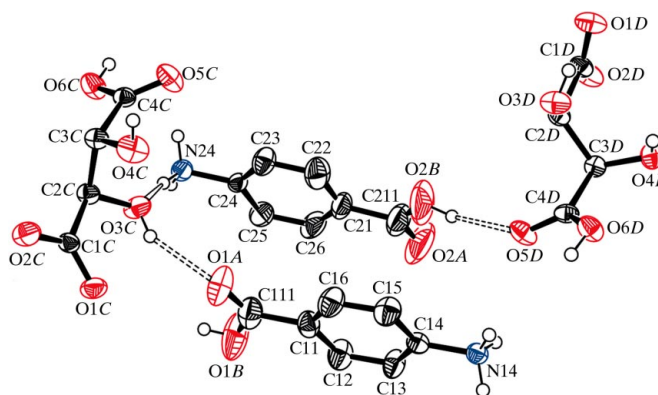


Figure 1

The molecular structure of (I), showing the atom-numbering scheme. Displacement ellipsoids are drawn at the 50% probability level and H atoms not involved in the hydrogen bonds (dashed lines) have been omitted for clarity.

twisting are 1.1 (2) and 6.8 (2)° in (I), and 3.0 (4) and 4.3 (4)° in (II).

As discussed above, the structure–extension property of PABA *via* hydrogen bonds is recognized as a possible tool for promoting cocrystallization, with the aim of designing noncentrosymmetric organic materials (Etter & Frankenbach, 1989). However, among the many reported adducts of PABA, only a few have been found to crystallize in noncentrosymmetric space groups (only four out of 27 complexes of PABA adducts in the CSD), and complex (I) is another such case.

In (II), the bond distances and angles (Table 3) are in agreement with the reported values (Lai & Marsh, 1967). Even though the molecular structure of (II) is already known, the aim of the present work is to elucidate the structure with precision, and to study the crystal packing of the molecule *via* hydrogen bonds and their visualization through graph-set notation (Etter *et al.*, 1990; Bernstein *et al.*, 1995).

As discussed in our previous publication (Athimoolam & Natarajan, 2006), head-to-tail hydrogen-bonding association (head = $\text{NH}_2/\text{NH}_3^+$ and tail = COOH) and carboxyl group dimerization are characteristic interactions found between the PABA residues in many PABA complexes in the CSD. In (I), these interactions are observed through the anions because of dominant hydrogen-bonding sites in the tartrates, and correspondingly the crystal packing can be described by an intricate three-dimensional hydrogen-bonding network (Fig. 3). In (II), head-to-tail interaction is seen through a discrete $D_1^1(2)$ motif *via* an $\text{N14}\cdots\text{O2A}$ hydrogen bond and carboxyl group

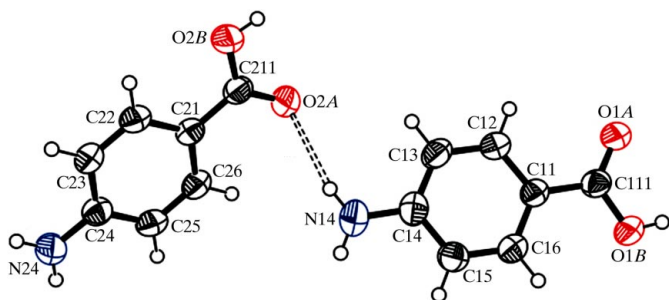


Figure 2

The molecular structure of (II), showing the atom-numbering scheme. Displacement ellipsoids are drawn at the 50% probability level and H atoms are shown as small spheres of arbitrary radii. Hydrogen bonds are shown as dashed lines.

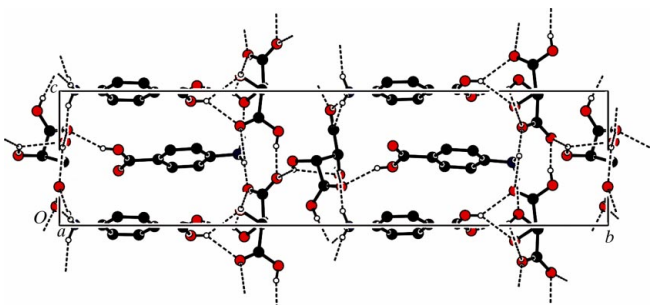


Figure 3

A packing diagram for (I), viewed down the *a* axis. Hydrogen bonds are shown as dashed lines.

dimerization is observed through centrosymmetrically related $R_2^2(8)$ motifs (in both residues in the asymmetric unit) around the inversion centres of the unit cell. Hence, in short, the crystal packing of (II) can be readily described with three primary motifs [two $R_2^2(8)$ and one $D_1^1(2)$] and two discrete secondary motifs [$D_2^2(7)$ and $D_3^3(19)$] (Table 3 and Fig. 4).

Alternate hydrophobic and hydrophilic layers are observed in (I) as a result of the column-like arrangement of the aromatic rings of the cations and the anions. Each tartrate anion forms a self-association of $S(5)$ motif *via* $\text{O}—\text{H}\cdots\text{O}$ intramolecular bonds. Even though tartrates form extensive intermolecular hydrogen bonds between themselves and with PABA, it is more sensible to discuss the characteristic

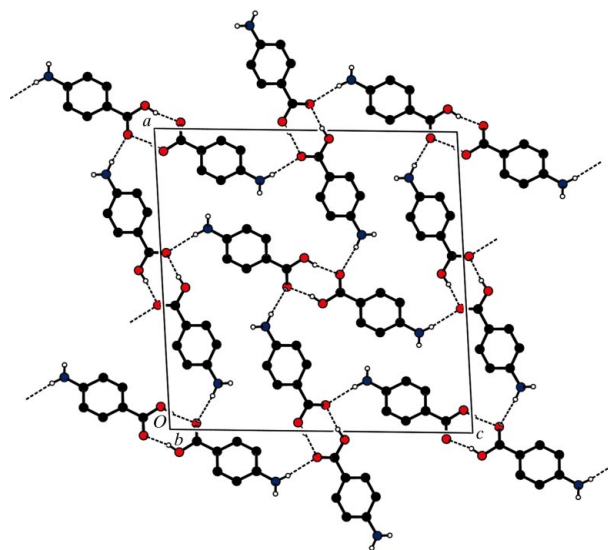


Figure 4

A packing diagram for (II), viewed down the *b* axis. Hydrogen bonds are shown as dashed lines.

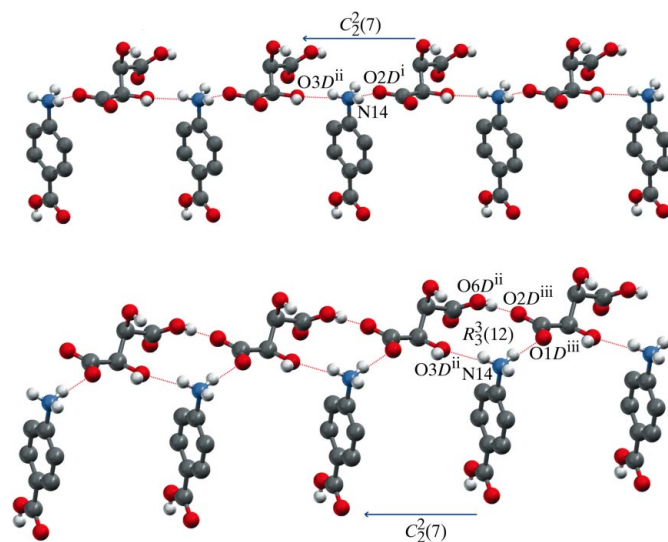


Figure 5

A view of the cations in (I) connected through the tartrate anions, showing the $C_2^2(7)$ chain motifs and $R_3^3(12)$ ring motifs. Hydrogen bonds are shown as dashed lines. [Symmetry codes: (i) $x, y, z - 1$; (ii) $x + 1, y, z$; (iii) $x + 1, y, z - 1$.]

hydrogen-bonding features than all the intricate hydrogen bonds (Table 4). The NH_3^+ group of the cationic residues of (I) and (II) form two sets of $C_2^2(7)$ chain motifs through the tartrate anions *via* $\text{N}-\text{H}\cdots\text{O}$ hydrogen bonds. Also, the tartrate anions are themselves connected *via* $\text{O}-\text{H}\cdots\text{O}$ bonds of another $C_2^2(7)$ chain motif. One of the two $C_2^2(7)$ chain motifs of the $\text{N}-\text{H}\cdots\text{O}$ hydrogen bonds and the $\text{O}-\text{H}\cdots\text{O}$ $C_2^2(7)$ chain motif lead to a ring of $R_3^3(12)$ motif in both cationic residues (Fig. 5). Fig. 6 shows the aggregation of the tartrates through $\text{O}-\text{H}\cdots\text{O}$ chain motifs of $C_1^1(6)$ and $C_1^1(7)$ running along the a and c axes of the unit cell, respectively. These chain motifs form a closed secondary $R_4^4(22)$ ring motif in both anions.

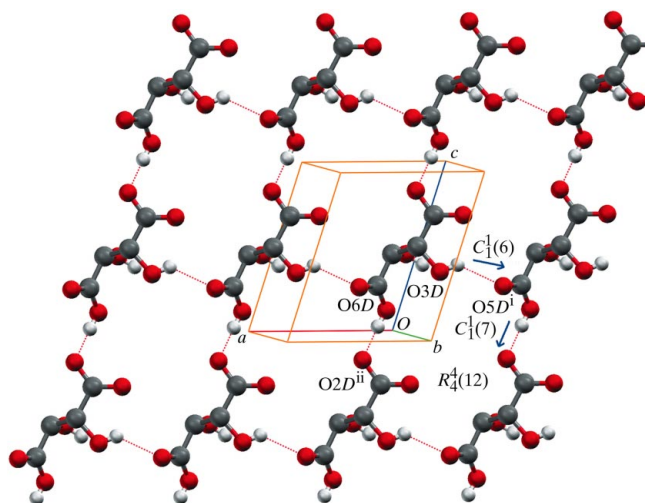


Figure 6
A view showing the aggregation of anions in (I) through the primary $C_1^1(6)$ and $C_1^1(7)$ tartrate graph-set motifs propagating along the a and c axes, respectively, and the secondary $R_4^4(22)$ ring motif. Hydrogen bonds are shown as dashed lines. [Symmetry codes: (i) $x - 1, y, z$; (ii) $x, y, z - 1$.]

Experimental

Compound (I) was crystallized from an aqueous solution containing 4-aminobenzoic acid and (2*R*,3*R*)-tartaric acid in a 1:1 stoichiometric ratio at room temperature by slow evaporation. Compound (II) was crystallized from a saturated aqueous solution of 4-aminobenzoic acid.

Compound (I)

Crystal data

$\text{C}_7\text{H}_8\text{NO}_2^+ \cdot \text{C}_4\text{H}_5\text{O}_6^-$ $V = 1225.0$ (12) \AA^3
 $M_r = 287.22$ $Z = 4$
 Monoclinic, $P2_1$ Mo $K\alpha$ radiation
 $a = 6.021$ (4) \AA $\mu = 0.14$ mm^{-1}
 $b = 28.789$ (11) \AA $T = 293$ (2) K
 $c = 7.426$ (5) \AA $0.22 \times 0.15 \times 0.13$ mm
 $\beta = 107.89$ (4)°

Data collection

Nonius MACH-3 sealed-tube diffractometer 2721 independent reflections
 Absorption correction: ψ scan 2127 reflections with $I > 2\sigma(I)$
 (North *et al.*, 1968) $R_{\text{int}} = 0.091$
 $T_{\text{min}} = 0.930$, $T_{\text{max}} = 0.981$ 3 standard reflections
 3083 measured reflections frequency: 60 min
 intensity decay: none

Refinement

$R[F^2 > 2\sigma(F^2)] = 0.039$ 1 restraint
 $wR(F^2) = 0.106$ H-atom parameters constrained
 $S = 1.08$ $\Delta\rho_{\text{max}} = 0.29$ e \AA^{-3}
 2721 reflections $\Delta\rho_{\text{min}} = -0.28$ e \AA^{-3}
 371 parameters

Table 1

Selected geometric parameters (\AA , °) for (I).

$\text{C111}-\text{O1A}$	1.196 (7)	$\text{C1C}-\text{O2C}$	1.261 (5)
$\text{C111}-\text{O1B}$	1.318 (7)	$\text{C4C}-\text{O5C}$	1.202 (5)
$\text{C14}-\text{N14}$	1.464 (6)	$\text{C4C}-\text{O6C}$	1.306 (5)
$\text{C211}-\text{O2A}$	1.205 (10)	$\text{C1D}-\text{O1D}$	1.232 (5)
$\text{C211}-\text{O2B}$	1.344 (10)	$\text{C1D}-\text{O2D}$	1.276 (5)
$\text{C24}-\text{N24}$	1.476 (5)	$\text{C4D}-\text{O5D}$	1.219 (5)
$\text{C1C}-\text{O1C}$	1.236 (5)	$\text{C4D}-\text{O6D}$	1.301 (5)
$\text{C12}-\text{C11}-\text{C111}-\text{O1B}$	1.3 (7)	$\text{C22}-\text{C21}-\text{C211}-\text{O2B}$	6.2 (8)

Table 2

Hydrogen-bond geometry (\AA , °) for (I).

$D-\text{H}\cdots A$	$D-\text{H}$	$\text{H}\cdots A$	$D\cdots A$	$D-\text{H}\cdots A$
$\text{O1B}-\text{H1B}\cdots\text{O5C}^{\text{i}}$	0.82	2.20	2.901 (6)	143
$\text{O1B}-\text{H1B}\cdots\text{O4C}^{\text{i}}$	0.82	2.25	2.949 (6)	143
$\text{N14}-\text{H14A}\cdots\text{O2D}^{\text{ii}}$	0.89	1.91	2.790 (5)	170
$\text{N14}-\text{H14B}\cdots\text{O3D}^{\text{i}}$	0.89	1.93	2.788 (4)	163
$\text{N14}-\text{H14C}\cdots\text{O1D}^{\text{iii}}$	0.89	1.81	2.687 (4)	168
$\text{O2B}-\text{H2B}\cdots\text{O5D}$	0.82	2.20	2.914 (6)	145
$\text{N24}-\text{H24A}\cdots\text{O2C}^{\text{iv}}$	0.89	2.63	3.490 (5)	164
$\text{N24}-\text{H24C}\cdots\text{O3C}$	0.89	1.92	2.787 (5)	166
$\text{N24}-\text{H24B}\cdots\text{O1C}^{\text{v}}$	0.89	1.89	2.737 (5)	159
$\text{O3C}-\text{H3C}\cdots\text{O1A}$	0.82	2.11	2.841 (5)	149
$\text{O4C}-\text{H4C}\cdots\text{O1C}^{\text{vi}}$	0.82	2.12	2.877 (5)	154
$\text{O6C}-\text{H6C}\cdots\text{O2C}^{\text{v}}$	0.82	1.80	2.608 (4)	171
$\text{O3D}-\text{H3D}\cdots\text{O5D}^{\text{vi}}$	0.82	2.11	2.715 (4)	131
$\text{O4D}-\text{H4D}\cdots\text{O2C}^{\text{vii}}$	0.82	2.06	2.782 (4)	146
$\text{O6D}-\text{H6D}\cdots\text{O2D}^{\text{ii}}$	0.82	1.70	2.515 (4)	175

Symmetry codes: (i) $x + 1, y, z$; (ii) $x, y, z - 1$; (iii) $x + 1, y, z - 1$; (iv) $x + 1, y, z + 1$; (v) $x, y, z + 1$; (vi) $x - 1, y, z$; (vii) $-x, y - \frac{1}{2}, -z$.

Compound (II)

Crystal data

$\text{C}_7\text{H}_7\text{NO}_2$ $V = 1327.06$ (13) \AA^3
 $M_r = 137.14$ $Z = 8$
 Monoclinic, $P2_1/n$ Mo $K\alpha$ radiation
 $a = 18.5712$ (8) \AA $\mu = 0.10$ mm^{-1}
 $b = 3.8431$ (3) \AA $T = 293$ (2) K
 $c = 18.6321$ (9) \AA $0.23 \times 0.14 \times 0.12$ mm
 $\beta = 93.670$ (11)°

Data collection

Nonius MACH-3 sealed-tube diffractometer 2845 independent reflections
 1746 reflections with $I > 2\sigma(I)$
 Absorption correction: ψ scan $R_{\text{int}} = 0.038$
 (North *et al.*, 1968) 3 standard reflections
 $T_{\text{min}} = 0.945$, $T_{\text{max}} = 0.985$ frequency: 60 min
 3787 measured reflections intensity decay: none

Refinement

$R[F^2 > 2\sigma(F^2)] = 0.066$ 183 parameters
 $wR(F^2) = 0.227$ H-atom parameters constrained
 $S = 1.17$ $\Delta\rho_{\text{max}} = 0.37$ e \AA^{-3}
 2845 reflections $\Delta\rho_{\text{min}} = -0.27$ e \AA^{-3}

Table 3

Selected geometric parameters (Å, °) for (II).

C111—O1A	1.230 (4)	C211—O2A	1.254 (4)
C111—O1B	1.318 (4)	C211—O2B	1.298 (4)
C14—N14	1.372 (5)	C24—N24	1.372 (5)
C16—C11—C111—O1B	−1.3 (5)	C22—C21—C211—O2B	−3.0 (6)

Table 4

Hydrogen-bond geometry (Å, °) for (II).

<i>D</i> —H... <i>A</i>	<i>D</i> —H	H... <i>A</i>	<i>D</i> ... <i>A</i>	<i>D</i> —H... <i>A</i>
O1B—H1B...O1A ⁱ	0.82	1.83	2.650 (4)	172
N14—H14A...O2A	0.86	2.57	3.369 (5)	154
O2B—H2B...O2A ⁱⁱ	0.82	1.81	2.616 (4)	166
N24—H24A...O1A ⁱⁱⁱ	0.86	2.13	2.969 (4)	165

Symmetry codes: (i) $-x+2, -y, -z+1$; (ii) $-x+1, -y, -z+1$; (iii) $x-\frac{1}{2}, -y+\frac{1}{2}, z+\frac{1}{2}$.

All H atoms were positioned geometrically and refined using a riding model, with C—H = 0.93 (aromatic CH) and 0.98 Å (—CH), O—H = 0.82 Å and N—H = 0.89 Å, and with $U_{\text{iso}}(\text{H}) = 1.2\text{--}1.5U_{\text{eq}}(\text{parent})$. In compound (I), in addition to the 2721 unique reflections, 109 Friedel pairs were measured. However, owing to the absence of atoms with significant anomalous dispersion effects, these data were merged.

For both compounds, data collection: *CAD-4 EXPRESS* (Enraf-Nonius, 1994); cell refinement: *CAD-4 EXPRESS*; data reduction: *XCAD4* (Harms & Wocadlo, 1995); program(s) used to solve structure: *SHELXTL/PC* (Bruker, 2000); program(s) used to refine structure: *SHELXTL/PC*; molecular graphics: *ORTEP-3* (Farrugia, 1997), *Mercury* (Version 1.4.1; Macrae *et al.*, 2006) and *PLATON* (Spek, 2003); software used to prepare material for publication: *SHELXTL/PC*.

The authors thank the Department of Science and Technology, Government of India, for establishing the Single-

Crystal Diffractometer facility at the School of Physics, Madurai Kamaraj University, Madurai, through the FIST programme. The authors also thank the UGC for the DRS programme.

Supplementary data for this paper are available from the IUCr electronic archives (Reference: AV3090). Services for accessing these data are described at the back of the journal.

References

- Allen, F. H. (2002). *Acta Cryst.* **B58**, 380–388.
- Athimoolam, S. & Natarajan, S. (2006). *Acta Cryst.* **C62**, o612–o617.
- Bernstein, J., Davis, R. E., Shimoni, L. & Chang, N.-L. (1995). *Angew. Chem. Int. Ed. Engl.* **34**, 1555–1573.
- Bruker (2000). *SHELXTL/PC*. Version 6.10. Bruker AXS Inc., Madison, Wisconsin, USA.
- Enraf-Nonius (1994). *CAD-4 EXPRESS*. Version 5.1/1.2. Enraf-Nonius, Delft, The Netherlands.
- Etter, M. C. & Frankenbach, G. A. (1989). *Chem. Mater.* **1**, 10–12.
- Etter, M. C., MacDonald, J. C. & Bernstein, J. (1990). *Acta Cryst.* **B46**, 256–262.
- Farrugia, L. J. (1997). *J. Appl. Cryst.* **30**, 565.
- Gracin, S. & Fischer, A. (2005). *Acta Cryst.* **E61**, o1242–o1244.
- Harms, K. & Wocadlo, S. (1995). *XCAD4*. University of Marburg, Germany.
- Hu, Z., Liu, J., Shen, L., Xu, D. & Xu, Y. (2002). *J. Chem. Crystallogr.* **32**, 525–527.
- Lai, T. F. & Marsh, R. E. (1967). *Acta Cryst.* **22**, 885–893.
- Le Fur, Y. & Masse, R. (1996). *Acta Cryst.* **C52**, 2183–2185.
- Lynch, D. E., Smith, G., Byriel, K. A. & Kennard, C. H. L. (1992). *Acta Cryst.* **C48**, 533–536.
- Macrae, C. F., Edgington, P. R., McCabe, P., Pidcock, E., Shields, G. P., Taylor, R., Towler, M. & van de Streek, J. (2006). *J. Appl. Cryst.* **39**, 453–457.
- North, A. C. T., Phillips, D. C. & Mathews, F. S. (1968). *Acta Cryst.* **A24**, 351–359.
- Osgood, P. J., Moss, S. H. & Davies, D. J. (1982). *J. Invest. Dermatol.* **79**, 354–357.
- Pant, A. K. (1965). *Acta Cryst.* **19**, 440–448.
- Robinson, F. A. (1966). *The Vitamin Co-factors of Enzyme Systems*, pp. 541–662. London: Pergamon.
- Spek, A. L. (2003). *J. Appl. Cryst.* **36**, 7–13.
- Tordjman, I., Masse, R. & Guitel, J. C. (1988). *Acta Cryst.* **C44**, 2057–2059.
- Wang, R., Hong, M. C., Luo, J., Jiang, F., Han, L., Lin, Z. & Cao, R. (2004). *Inorg. Chim. Acta*, **357**, 103–108.